www.czasopisma.pan.pl PAN POLSKA AKADEMIA NAUK www.journals.pan.pl

Arch. Min. Sci. **65** (2020), 2, 317-335

Electronic version (in color) of this paper is available: http://mining.archives.pl

DOI 10.24425/ams.2020.133195

JAMSHID SHAKERI[1], BEHSHAD JODEIRI SHOKRI[1], HESAM DEHGHANI[1*]

PREDICTION OF BLAST-INDUCED GROUND VIBRATION USING GENE EXPRESSION PROGRAMMING (GEP), ARTIFICIAL NEURAL NETWORKS (ANNS), AND LINEAR MULTIVARIATE REGRESSION (LMR)

In this paper, an attempt was made to find out two empirical relationships incorporating linear multivariate regression (LMR) and gene expression programming (GEP) for predicting the blast-induced ground vibration (BIGV) at the Sarcheshmeh copper mine in south of Iran. For this purpose, five types of effective parameters in the blasting operation including the distance from the blasting block, the burden, the spacing, the specific charge, and the charge per delay were considered as the input data while the output parameter was the BIGV. The correlation coefficient and root mean squared error for the LMR were 0.70 and 3.18 respectively, while the values for the GEP were 0.91 and 2.67 respectively. Also, for evaluating the validation of these two methods, a feed-forward artificial neural network (ANN) with a 5-20-1 structure has been used for predicting the BIGV. Comparisons of these parameters revealed that both methods successfully suggested two empirical relationships for predicting the BIGV in the case study. However, the GEP was found to be more reliable and more reasonable.

Keywords: Blasting; Ground vibration; Gene expression programing; Linear multivariate regression; Sarcheshme copper mine

1. Introduction

Despite all achievements and significant developments that have taken place in drilling and rock cutting industries, the blasting operation is still the main important method for grinding and displacing the rocks in the mining activities [1]. Moreover, some of the most significant environmental issues such as flyrock, air blast, noises, back breaks, and blast-induced ground vibration (BIGV) causing by the blasting operations. Among these undesirable side effects, the

[1] DEPARTMENT OF MINING ENGINEERING, HAMEDAN UNIVERSITY OF TECHNOLOGY, HAMEDAN, IRAN

* Corresponding Author: dehghani@hut.ac.ir

BIGV is recognized as an adverse phenomenon that results from escaping some of the explosive energy, 40%, through the surface soil and the bedrock. Due to its' vast effects on above-ground and below-ground structures, neighboring rock masses, roads, slopes, railways, buried pipelines, and transmission lines, it is worth developing appropriate predictive methods of the BIGV to minimize the further environmental risks [2]. Investigation of the frequency and peak particles (PPV) plays a critical role in the BIGV studies. Hence, predicting the BIGV and the PPV are given careful considerations during the last decades and as a consequence, several analytical, mathematical, statistical, and intelligent methods have been presented and developed.

Khandelwal and Singh presented the application of neural network (NN) for predicting the GV and vibration frequency considering all parameters affecting the rock mass, blasting properties, and blast design. To evaluate the presented methodology, they further compared their prediction results to conventional statistical procedures using the artificial neural networks (ANNs). For this purpose, their network was trained with a total of 150 datasets containing 458 epochs before being tested by 20 datasets. They also applied a comprehensive statistical analysis. The comparison results between the NN and the statistical analysis revealed that NN could predict the PPV in a better way [1]. The ANN was also applied by Monjezi et al. to evaluate the BIGV resulting from a blasting operation in building a dame, Siah-Bisheh, in the north of Iran [3]. Dindarloo used gene expression programming (GEP) to predict the PPV. They used nine types of different variables as input data for predicting the vibration frequencies at different distances to the blast face. The high value of the coefficient of determination, as well as low value of the mean absolute prediction error (MAPE), verified the efficiency of employing the GEP in predicting the reliable PPV measurements [4]. Hajihasani et al. presented a hybrid algorithm of ANN coupled with particle swarm optimization (PSO) for the BIGV and the air blast. Their results showed that the proposed model can be considered as a powerful method in predicting the BIGV and the air blast [5]. Armaghani et al. used a combination of the adaptive neuro-fuzzy inference system (ANFIS) and the ANNs for predicting the BIGV in mines. For this purpose, they considered the measured values of blasting parameters and the resultant the BIGV for a total of 109 blasting operations in the Johor Granite Mine (Malaysia). They found that the ANFIS could provide the best performance for predicting the BIGV, as compared to other prediction methods [6]. Faradanbeh et al. presented a GEP-based prediction model for estimating the BIGV in a granite mine in Malaysia. For this purpose, they evaluated 102 blasting operations and measured the blasting parameters. To find out the capability of the GEP model for predicting the GV, a nonlinear multivariate regression (NMR) was also applied on the same dataset, with the results highlighting the higher accuracy of the GEP model [2]. In another research, Hasanipanah et al. checked the applicability of genetic algorithm (GA) for proposing a new prediction model for estimating the BIGV in the vicinity of Bakhtiari Dam (Iran). With a comparison between the GA and multiple empirical prediction models, it was concluded that the GA had better results in this case [7]. Faradanbeh and Monjezi investigated the prediction and minimization of BIGV in Golgohar Iron Mine applying the GEP and cuckoo optimization algorithm (COA). They suggested that the development of the COA model could significantly reduce the PPV values [8]. Sheykhi et al. presented a hybrid model incorporating support vector regression (SVR) and fuzzy C-means Clustering (FCM) for predicting the BIGV. The model was developed based on the blasting data collected at Sarcheshmeh copper mine (Iran). The results revealed that the SVR technique was more efficient and more accurate than the existing empirical equation and that the data clustering plays an effective role in the accurate prediction of BIGV [9].

Although the literature review showed that artificial intelligence (AI) techniques have intensively been developed and proposed for estimating BIGV [10-12], their efficiency is different. Furthermore, the BIGV and its effects are different because of depending on the blast design parameters, geological conditions as well as the location of each mine. The most advantage of the previous studies is to consider the effect of different parameters of the drilling pattern on the BIGV. But few studies have attempted to minimize this phenomenon in addition to predicting it. Considering the losses and damages caused by the BIGV and its importance from the viewpoint of many researchers, the undesirable BIGV mechanism and its influential parameters in the Sarcheshmeh copper mine has been studied in this paper. For achieving this aim, a mathematical relationship was proposed by using the GEP.

2. Methodology

In this paper, the BIGV has been predicted by using the linear regression, artificial neural networks and the GEP, which are discussed in the following subsections.

2.1. Linear Regression Model

The general linear model (GLM) or multivariate regression is a statistical linear model which is written as equation (1):

$$C = Bx + \varepsilon \tag{1}$$

Where:

C — is a dependent value;
x — is an independent value;
ε — error of the model.

This method is applied when one dependent variable is determined by only one independent variable.

2.1.1. Linear multivariate Regression Model

The linear multivariate regression (LMR) is a generalization of simple linear regression to the case of more than one independent variable, and a special case of general linear models, restricted to one dependent variable. In this paper, the dependent variable which assumed as PPV may depend on n independent variables (x). Equation (2) expresses a LMR with n regression variables [13]:

$$C = \beta_0 + \beta_1 x_1 + \ldots + \beta_n \beta_n + \varepsilon \tag{2}$$

where:

ε — error of the model;
$j = 0, 1, \ldots, n$ and β_j are the regression coefficients.

In fact, the prediction process using this model resembles a super plane in an n-dimensional space of the regression variables x_j. On the other hand, one may consider prediction models of

more complex structures (nonlinear) than those expressed by Equation (3). For instance, in the following model [13]:

$$C = \beta_0 + \beta_1 x_1 + \beta_2 x_2^3 + \beta_3 e^{x_3} + \beta_4 x_1 x_2 + \varepsilon \tag{3}$$

In order to simplify the analysis of the above equation, which is nonlinear, one can simply substitute its variables with linear variables. Accordingly, taking $z_1 = x_1$, $z_2 = x_2^3$, $z_3 = e^{x_3}$, and $z_4 = x_1 x_2$. Equation (4) will take the following form to predict the PPV values:

$$C = \beta_0 + \beta_1 z_1 + \beta_2 z_2 + \beta_3 z_3 + \beta_4 z_4 + \varepsilon \tag{4}$$

2.2. Gene expression programming (GEM)

The gene expression programing (GEP) refers to a methodology for developing computer programs and mathematical modeling based on evolutionary computations inspired by the natural evolution phenomena. This method was coined by Ferreira in 1999 and officially released in 2001 [14]. The GEP integrated the ideas of the two preceding legacy algorithms in an attempt to cover their weaknesses. In this methodology, the genotype of the chromosomes possesses a linear structure, similar to the case with GA. On the other hand, the phenotype of the chromosomes exhibits a tree structure with variable length and size, similar to the case with genetic programing (GP). Karva code is the language of choice for GEP, and multiple genes are used to capture the multiple structures of chromosomes and the ability to generate subtrees, providing the algorithm with better compatibility and performance [14]. The flowchart of the GEP is shown in Figure 1. According to this figure, the algorithm begins with random generation of an initial population (chromosomes). The generated population is then expressed followed by evaluating each individual based on an evaluation function, with a selection process then performed based on the evaluation results. Applying particular modifications to the selected individuals, a new population of selected individuals with new characteristics is generated. The new population will then repeat the mentioned procedure and this process continue until an appropriate solution is achieved (Fig. 1) [14]. Because of the many advantages of the GEP, this method is used to solve the optimization problems in various sciences such as mining, economics, etc. [15-17].

2.3. Artificial Neural Networks (ANNs)

ANNs have different layers including input, hidden and output layers in their structure. Each layer consists of one to several neurons according to the position of the layer. The number of neurons in the input layer denotes the number of parameters that are used for the prediction while the number of neurons in the output layer represents the number of variables to be predicted. The appropriate number of neurons in hidden layers will generally be obtained during a trial and error process. Neurons of a layer are linked to the neighboring layer neurons by interconnection weights. Initial interconnection weights are randomly generated. Pairs of inputs and outputs are fed to the ANNs where inputs are multiplied by interconnection weights and then the products are added together to obtain the corresponding predicted output(s). The predicted output is then compared to the related actual output, which has already been fed to the network; the error is propagated backward to find the value of the weights that minimize differences between the actual output and the predicted output in the output layer. When a back-propagation algorithm is

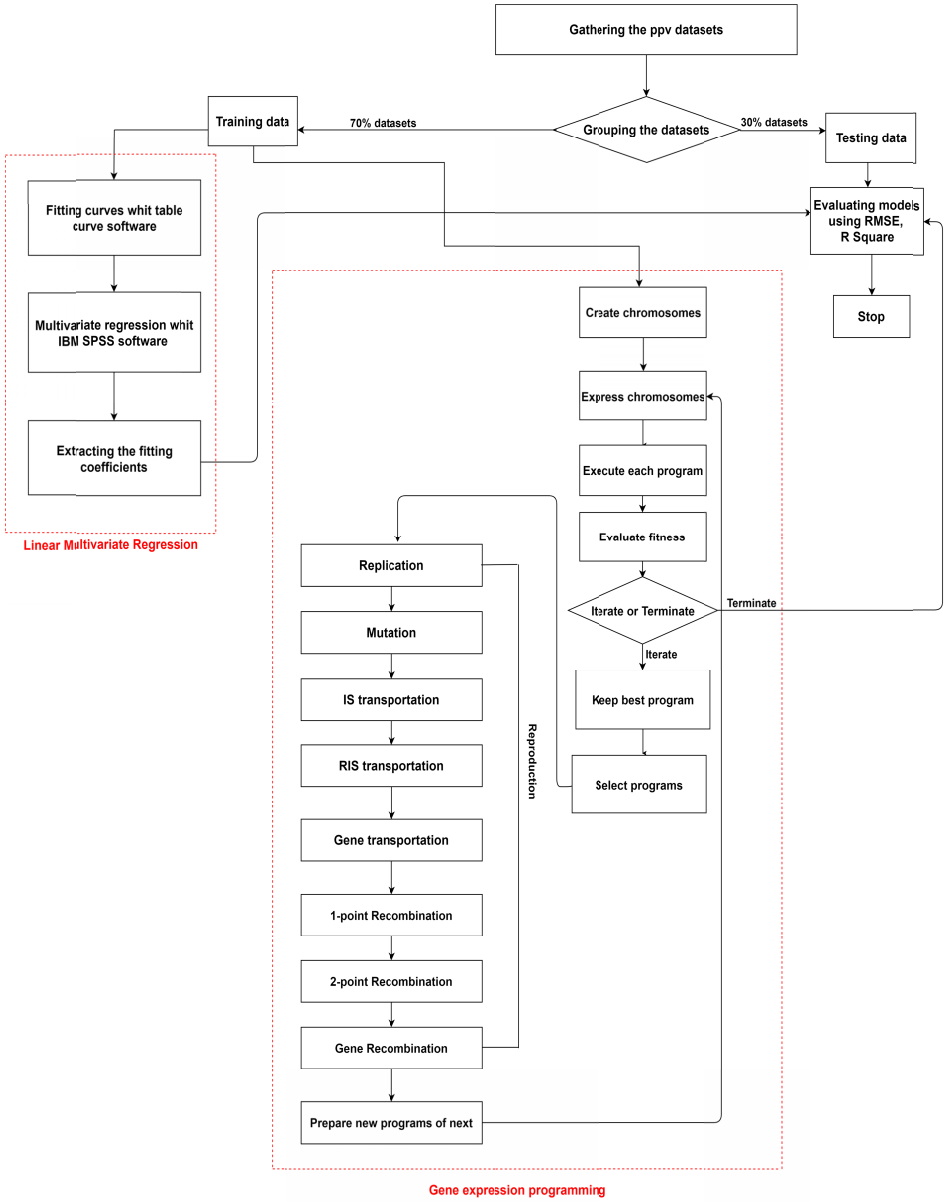

Fig. 1. Flowcharts of GEP and LMR

applied, methods exist to terminate training, such as measuring MSE and the number of learning courses (epochs). Another validation method after each learning epoch is called the early stopping method [18]. This method can prevent a network from over-learning (or over-fitting). In this paper, the MSE method was used to prevent over-fitting. To make use of the early stopping method, the database was divided into three subsets: training, validation, and test datasets.

3. Case study

Blast induced ground vibration was studied in one of the most important and largest copper mines in Iran. The Sarcheshmeh copper ore mine is situated 160 km southwest of Kerman city, Kerman province, in 55º 15' 13" longitude and 29º 57' 00" latitude. This mine is at 2500 m above sea level (Fig. 2). Geological reserve of the mine has been estimated to exceed 1.2 billion tons of sulfuric copper ore with an average grade of 0.7%. The mine is located in a cold desert climate region with an average precipitation of 550 mm per year. The temperature varies from –15° in winter to +32° in summer. The production units of the copper complex include the mine, the concentration, the melting, and refining, and the casting and leaching units. There are multiple copper exploitation sites, most of which are being operated as open-pit mines. Some of the mines have been active for the past 40 years. In some parts, the surface soil naturally contains high concentrations of copper and other heavy metals, such as zinc and lead. In this region, due to the open-pit mining of copper, blasting operation is used for grinding purposes, which is known to cause such consequences as GV, air vibration, over break, and fly rock. Accordingly, it is very important to investigate the blast-induced consequences, including BIGV, in the region.

Fig. 2. A view to the Sarcheshmeh Copper Mine

The ore body is oval shaped, covering an elliptical area of 2300 m × 1200 m from the southeast to the northwest, with an average depth of 1612 m [19]. The geology of the deposit is dominated by Eocene basic to intermediate volcanic rocks including trachybasalt, trachyandesite, and/or andesite. Mineralization at Sarcheshmeh deposit mainly forms stockworks and veins that are equally distributed between Eocene volcanic and Oligo-Miocene quartz diorite, quartz monzonite, and granodiorite units. There is a complex of series of magmatically related intrusives emplaced in the Tertiary Volcanics a short distance from the edge of an older near-batholithsized granodiorite mass [20]. The most significant sulfide minerals of the deposited include chalcocite, chalcopyrite, kaolinite, bornite, and molybdenite. The oxidized zone of the deposit is mainly

comprised of copperite, malachite and azurite. The pyrite is the most significant band mineral matter in the region. Figure 3 shows the geological map of the Sarcheshmeh deposit [21].

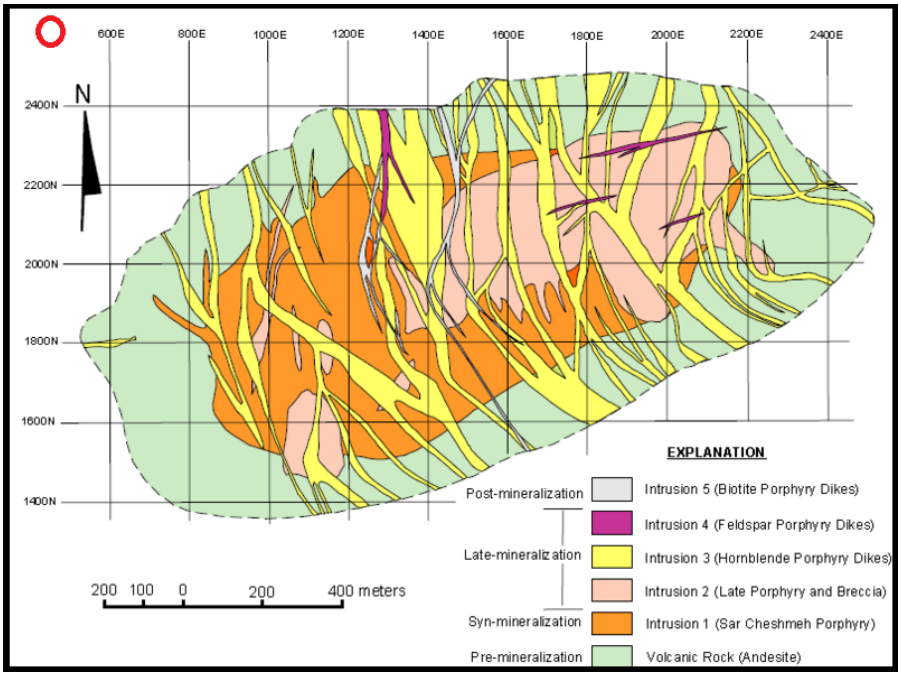

Fig. 3. Geological Map of the Sarcheshmeh porphyry copper mine [20]

The height and slope of working benches are 14 m and 62.5º, respectively. The angle of overall slope ranges from 32º to 34º. The diameter and depth of blast holes are mostly 0.200 and 15 m, respectively. ANFO is used as the main explosive. Pattern geometry is staggered. Drilling cuttings are used as stemming material [21]. In order to determine the amount of the BIGV in this mine, five main input parameters were selected from 113 blasting patterns, i.e. distance to blasting block, burden, spacing, specific charge, and charge per delay. The range of the input and output parameters is listed in Table 1. The box diagrams for the input data are also shown in Figure 4.

TABLE 1

Range of the datasets used for the model development

Parameter	Symbol	Change interval	Parameter type
Charge per Delay (Kg/ms)	A	1332-10985	Input data
Distance to blasting block (m)	F	133.02-2845.02	
Burden (m)	B	3-7.5	
Spacing (m)	S	4-11	
Specific charge (Kg/m^3)	P	0.116-0.226	
Peak Particle Velocity (mm/s)	PPV	0.49-39.15	Output data

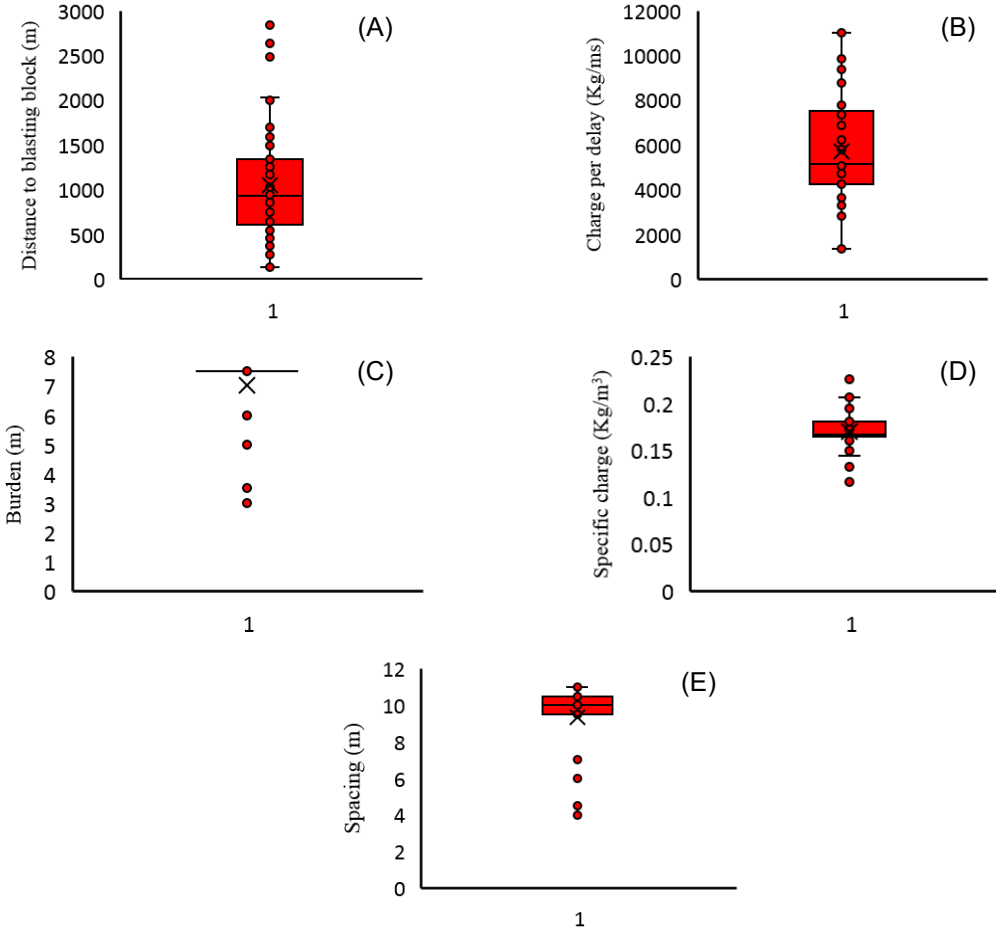

Fig. 4. Box diagrams of the input data: (A) distance to blasting block (m); (B) charge per delay (Kg/ms); (C) burden (m); (D) specific charge (Kg/m^3), and (E) spacing (m)

Afterward, to find the best statistical relationship between input and output data, the dataset has randomly been divided into training and validation data. For this, 70% of the data considered as training data while the rest of the data, 30%, was applied for validation of the suggested statistical relationship.

4. Statistical Analyses

4.1. Determining the statistical relationships

After describing the data, the best statistical relationships between each the input and the output data have been suggested by using the Table curve v.5.01 software which is one of the

most powerful statistical software for curve and surface fitting the data. These relationships have been selected based on their R-squared coefficients. The best statistical relationships, 15, have been presented in Table 2. Indeed, this analysis provides an opportunity to consider the inter-relationship between the input and output data in the further proposed relationship.

TABLE 2

Relationships between input variables and PPV

Row	Equation	Relationship between parameters
1	$x_1 = \frac{1}{A^2}$	$PPV \propto f(A)$
2	$x_2 = \frac{1}{F}$	$PPV \propto f(F)$
3	$x_3 = e^{-B}$	$PPV \propto f(B)$
4	$x_4 = \frac{\ln(P)}{P^2}$	$PPV \propto f(P)$
5	$x_5 = e^{S}$	$PPV \propto f(S)$
6	$x_6 = \frac{\ln(A)}{A} + \frac{\ln(F)}{F}$	$PPV \propto f(A \propto F)$
7	$x_7 = B^2 \times \ln(B) + B^{2.5}$	$PPV \propto f(A \propto B)$
8	$x_8 = \frac{1}{A} + \frac{1}{A^2}$	$PPV \propto f(A \propto P)$
9	$x_9 = S^{0.5} + \frac{\ln(S)}{S}$	$PPV \propto f(A \propto S)$
10	$x_{10} = \frac{\ln(F)}{F} + B^3$	$PPV \propto f(F \propto B)$
11	$x_{11} = \frac{1}{F} + P^{0.5} \times \ln(P)$	$PPV \propto f(F \propto P)$
12	$x_{12} = \frac{\ln(F)}{F} + \frac{\ln(S)}{S}$	$PPV \propto f(F \propto S)$
13	$x_{13} = B^2 \times \ln(B) + B^{2.5}$	$PPV \propto f(B \propto P)$
14	$x_{14} = S^{0.5} + \frac{\ln(S)}{S}$	$PPV \propto f(B \propto S)$
15	$x_{15} = S^{0.5} + \frac{\ln(S)}{S}$	$PPV \propto f(P \propto S)$

4.2. Suggesting a statistical relationship for prediction of PPV

After finding the best relationships between the input and the output data, each of the relationships has been considered as independent variables while the output was PPV. For finding the best relationship for prediction of PPV, comprehensive statistical analyses have been conducted by applying the IBM SPSS statistics software v.25 based on the LMR method. For this, the back-propagation method has been used to identify the best multivariate regression relationship

among the selected relationships. More than 8 relationships have been taken after these analyses (Table 3). To find out the best relationship, three statistical parameters were chosen as the best criteria: (1) R-square; (2) Adjusted R-square and (3) Root mean squared error (RMSE). The principal goal of this process was to specify a statistical relationship exhibiting the maximum values of R-square and adjusted R-square and the minimum value of RMSE. For this, all relationships were compared (See table 3). Comparison of the statistical parameters of the relationships, describing that the relationship no.5 is the best statistical relationship for predicting PPV. This relationship yields value of 0.714, 0.689, and 3.18 for the statistical parameters of R-square, adjusted R-Square, and RMSE respectively.

TABLE 3

Comparison of the statistical parameters of the models obtained using LMR

Model	R Square	Adjusted R Square	RMSE
1	0.714	0.668	3.68
2	0.714	0.673	3.66
3	0.714	0.677	3.63
4	0.714	0.682	3.61
5	0.714	0.689	3.18
6	0.712	0.686	3.57
7	0.707	0.687	3.58
8	0.705	0.688	3.56

Therefore, the best statistical relationship taken from the LMR is expressed as equation (5):

$$PPV = C_0 + C_1 x_{14} + C_2 x_4 + C_3 x_1 + C_4 x_{13} + C_5 x_3 + C_6 x_{11} + C_7 x_6 \tag{5}$$

where $C_0 - C_7$ denote the constants of the equation, with their values reported in Table 4.

TABLE 4

The values of the coefficients C_0 to C_7

C_0	C_1	C_2	C_3	C_4	C_5	C_6	C_7
–2.099	0.159	1.227	–4.479	–1.202	4.353	–0.527	1.768

Eventually, the best statistical relationship for predicting PPV which is a function of the distance to the blasting block, burden, spacing, specific charge, and charge per delay is expressed as follows (Eq. (6)):

$$\begin{aligned} PPV = {} & (-2.099) + \left(0.159 \times \left(S^{0.5} + \frac{\ln(S)}{S}\right)\right) + \left(1.227 \times \left(\frac{\ln(P)}{P^2}\right)\right) + \\ & \left(-4.479 \times \left(\frac{1}{A^2}\right)\right) + \left(-1.202 \times \left(B^2 \times \ln(B) + B^{2.5}\right)\right) + \left(4.353 \times \left(e^{-B}\right)\right) + \\ & \left(-0.527 \times \left(\frac{1}{F} + P^{0.5} \times \ln(P)\right)\right) + \left(1.768 \times \left(\frac{\ln(A)}{A} + \frac{\ln(F)}{F}\right)\right) \end{aligned} \tag{6}$$

Figure 5 demonstrates a histogram for the analysis of the modeling error. The modeling error distribution function is a normal function, confirming the regression test has been done correctly.

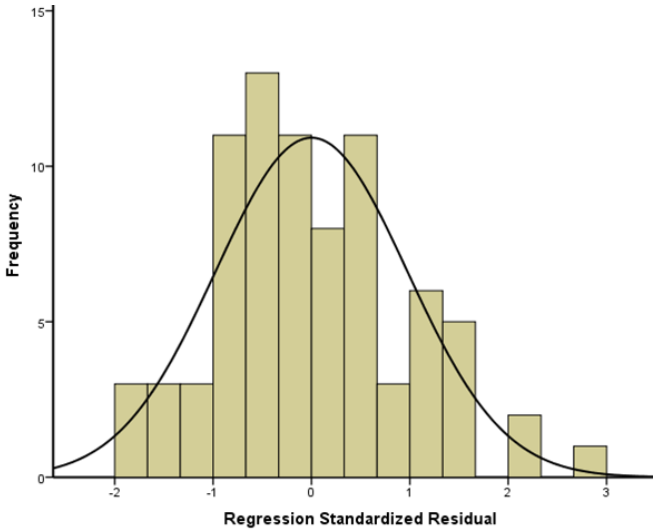

Fig. 5. Histogram for the analysis of the modeling error

5. GEP Model

In the present study, a GEP code was used to obtain the final relationship between the input data and the output data, PPV. The GEP modeling goes through five main steps; in this respect, the first step is to select a fitness evaluation function. In this study, the R-squared, RMSE, and MSE have been used as fitness function, and the best results were obtained with MSE as the fitness evaluation function. The relationships for expressing each of the fitness evaluation functions are shown in the following equations nos. (7) to (9):

$$MSE = \frac{1}{N}\sum_{i=1}^{N}(X_{ipred} - X_{imes})^2 \tag{7}$$

$$RMSE = \sqrt{\frac{1}{N}\sum_{i=1}^{N}(X_{ipred} - X_{imes})^2} \tag{8}$$

$$R^2 = 1 - \frac{\sum_{i=1}^{N}(X_{imes} - X_{ipred})^2}{\sum_{i=1}^{N}(X_{imes} - \bar{X})^2} \tag{9}$$

Where, X_{ipred} is the predicted PPV and X_{imes} is the measured PPV.

The second step is to select sets of terminals and functions to form chromosomes. The terminals were selected according to the model inputs and outputs. The inputs included the distance to the blasting block, burden, spacing, specific charge, and charge per delay, and the output parameter was the ground vibration. Following with the research, the most appropriate functions for obtaining the final equation have been determined in such a way to come with the best equation. The functions used in the modeling included {F = + , – , * , / , sqrt , x^2 , x^3 , x^(1/3) , 1/x , exp(x) , ln(x)}. The third step is related to the chromosome structure selection. As the fourth step, one should select the type of linking function; here we used a multiplication function to link the parameters. Finally, in the step 5, one should generate a set of genetic operators and rates. The parameters set in the software are tabulated in Table 5.

TABLE 5

The values of the parameters used for the GEP models

GEP parameters	**Model**				
	1	**2**	**3**	**4**	**5**
Fitness function	MSE	MSE	MSE	R-square	RMSE
Inversion rate	0.00546	0.00546	0.00546	0.00546	0.00546
IS transportation rate	0.00546	0.00546	0.00546	0.00546	0.00546
RIS transportation rate	0.00546	0.00546	0.00546	0.00546	0.00546
One-point recombination rate	0.00277	0.00277	0.00277	0.00277	0.00277
Two-point recombination rate	0.00277	0.00277	0.00277	0.00277	0.00277
Gene size	17	19	15	17	17
Head size	8	9	7	8	8
Tail size	9	10	8	9	9
Mutation rate	0.00138	0.00138	0.00138	0.00138	0.00138
Number of Chromosome	30	35	30	30	30
Number of genes	3	5	7	3	3
Gene recombination rate	0.00277	0.00277	0.00277	0.00277	0.00277
Gene transportation rate	0.00277	0.00277	0.00277	0.00277	0.00277
Training	%70	%70	%70	%70	%70
Validation	%30	%30	%30	%30	%30
Number of generation	10000	10000	10000	10000	10000

Lastly, the values of R-square and other parameters were obtained for the models built based on Table 5, which were known to have the best outputs among the investigated models. The results are shown in Table 6.

TABLE 6

Values of performance indicators for building the GEP models

Model	**Fitness function**	**Training**		**Testing**	
		R^2	**RMSE**	**R^2**	**RMSE**
1	MSE	0.68	3.36	0.91	2.67
2	MSE	0.66	3.53	0.87	3.68
3	MSE	0.67	3.39	0.84	3.06
4	R-Square	0.77	3.47	0.62	3.07
5	RMSE	0.65	3.49	0.88	2.72

According to Table 6, among the models constructed using the GEP, model 1 was the optimal one because of its higher R-squared value and lower RMSE, as compared to the other final four models. Model 1 was built based on a total of 80 data points as the training subset, with 33 datasets used to validate the model. Using the GEP algorithm, the expression tree corresponding to final model for predicting the PPV is shown in Figure 6, and Equation (10) presents the final relation extracted from the tree. Coefficients of this equation are listed in Table 7.

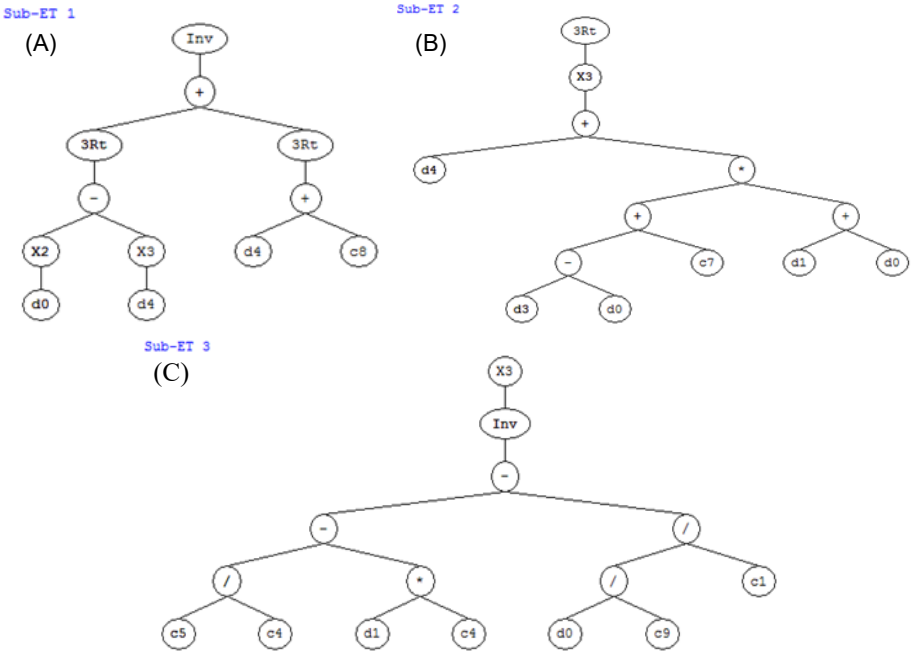

Fig. 6. The expression tree corresponding to model 1

$$ppv = \left(\frac{1}{\sqrt[3]{A^2 - S^3} + \sqrt[3]{S + C_8}} \right) \times$$

$$\times \sqrt[3]{\left(S + \left(\left((P - A) + C_7 \right) \times (F + A) \right) \right)^3} \times \left(\frac{1}{\left(\left(\frac{C_5}{C_4} \right) - (F \times C_4) \right) - \left(\frac{\frac{A}{C_9}}{C_1} \right)} \right)^3 \tag{10}$$

where C_1 – C_9, denote the constants of the equation, with their values reported in Table 7.

TABLE 7

The values of the coefficients C_0 to C_9

C_0	C_1	C_2	C_3	C_4	C_5	C_6	C_7	C_8	C_9
0.0	–4.78	0.0	0.0	–5.67	–6.34	0.0	4.54	7.36	–3.43

Eventually, the best GEP relationship for predicting PPV which is a function of the distance to the blasting block, burden, spacing, specific charge, and charge per delay is expressed as follows (Eq. (11)):

$$ppv = \left(\frac{1}{\sqrt[3]{A^2 - S^3} + \sqrt[3]{S + 7.36}}\right) \times \sqrt[3]{\left(S + \left(\left((P - A) + 4.54\right) \times (F + A)\right)\right)^3} \times \left(\frac{1}{\left(\left(\frac{-6.34}{-5.67}\right) - (F \times -5.67)\right) - \left(\frac{A}{\frac{-3.43}{-4.78}}\right)}\right)^3 \tag{11}$$

6. ANNs prediction

For finding the ability of GEP in predicting the PPV, the obtained results were compared with the results of the artificial neural network algorithm. As described before, this algorithm is so accurate and many researchers used it for predicting the various problems. For this purpose, a multi-layer perceptron (MLP) network was used. Although for reaching an appropriate architecture, MLP networks with one and two hidden layers were examined, it should be noted that a single hidden layer with enough neurons is generally sufficient to resolve a practical complex.

As mentioned before, five variables (burden, charge per delay, distance to blasting block, specific charge, and spacing) were considered as input parameters. As a result, the input layer of ANN structure had five neurons. However, the only variable that had to be predicted was the PPV, which meant that the output layer required only one neuron. To determine the optimal number of neurons in the hidden layer, after multiple instructions and tests of the network by various numbers of neurons in the hidden layer, 20 neurons were distinguished using a feed-forward ANN applying batch gradient descent with momentum back-propagation learning algorithm on the basis of RMSE. Therefore, the final structure of ANN was obtained as 5-20-1 (Fig. 7). The architecture of the obtained ANNs is presented in Table 8.

TABLE 8

Architecture of ANN model

Transfer Function	Model	R^2	RMSE
LOGSIG–LOGSIG–POSLIN (L-L-P)	5-20-1	0.88	2.81

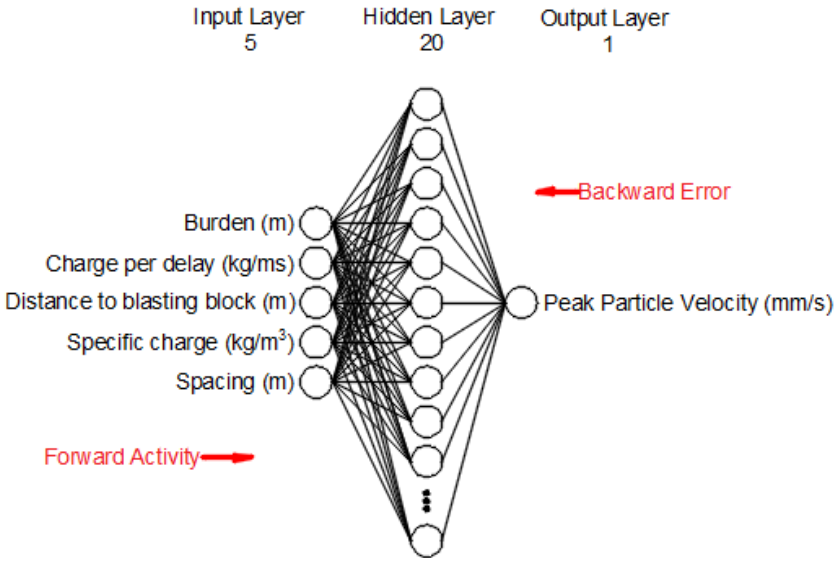

Fig. 7. the ANNs architecture with 5-20-1 (back propagation network)

7. Discussion

7.1. Validation

As mentioned, the main aim of this paper was to present two new relationships for predicting the PPV based on the parameters including the distance to the blasting block, the burden, the spacing, the specific charge, and the charge per delay. To propose the relationships, firstly, the data collected from the Sarcheshmeh copper mine were used to establish a database between the input and output data. Then, the best relationships between the PPV and each input were investigated by comprehensive statistical analyses. Subsequently, the GEP and LMR algorithms were applied to suggest the best relationships for predicting the PPV. Along with these algorithms, the ANN was also used to investigate the efficiency of the algorithms. The obtained results of these three methods were then compared based on the R-squared and RMSE values for training and validation stages. The GEP, LMR, and ANNs algorithms returned R-square values of 0.68, 0.71, and 0.67 for the training dataset respectively while they were 0.91, 0.70, and 0.89 for the validation dataset, as compared to the actually measured data, respectively (Figure 8). Moreover, the GEP, the LMR, and the ANNs algorithms gave RMSE values of 2.67, 3.18, and 2.81 for the validation dataset respectively. These results also prove that the GEP provides better results for the prediction of the PPV.

Figure 9 shows a cross plot of the measured data versus predicted values of PPV using the GEP, the ANN and the LMR algorithms. Based on this figure, the best predictions were obtained using the GEP algorithm. The amount of mean absolute error (MSE), absolute relative error (ARE), average absolute relative error (AARE) and root mean square error (RMSE), were compared for GEP, LMR and ANNs in Figure 10.

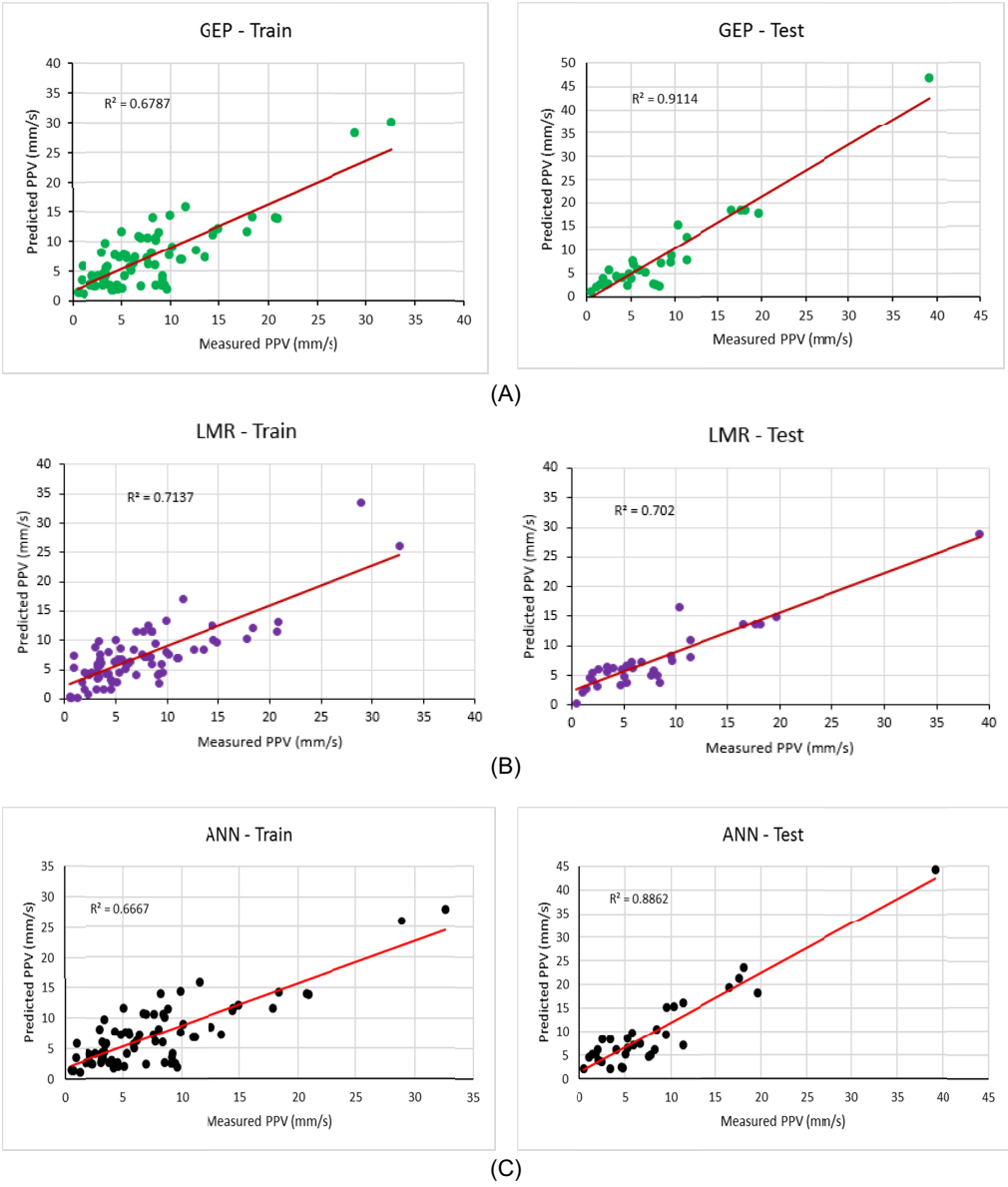

Fig. 8. The values of R-squared for: (A) GEP algorithm, (B) LMR algorithm, and (C) ANNs algorithm

7.2. Sensitivity analysis

A useful concept has been proposed to identify the significance of each "cause" factors (the input data) on the "effect factor" (the output). This enables us to hierarchically recognize the most sensitive factors affecting the PPV. For achieving this aim, the tornado graph was conducted. In

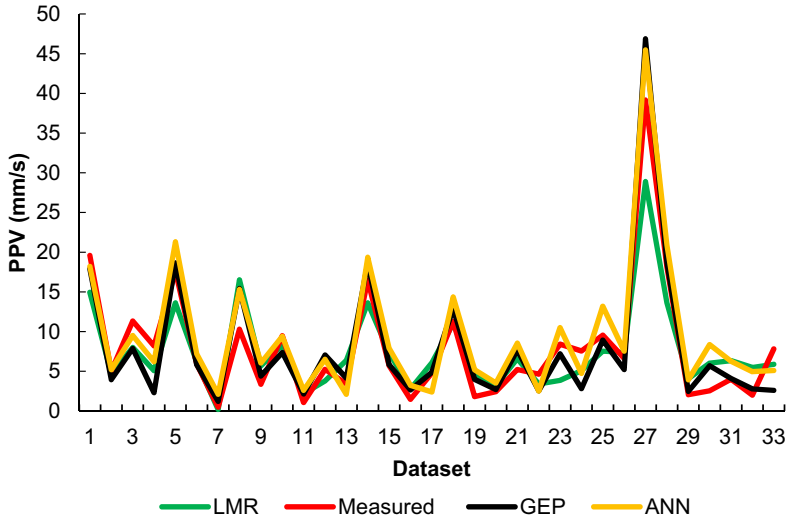

Fig. 9. Comparison of the measured PPV versus predicted PPV using the GEP, ANNs, and LMR

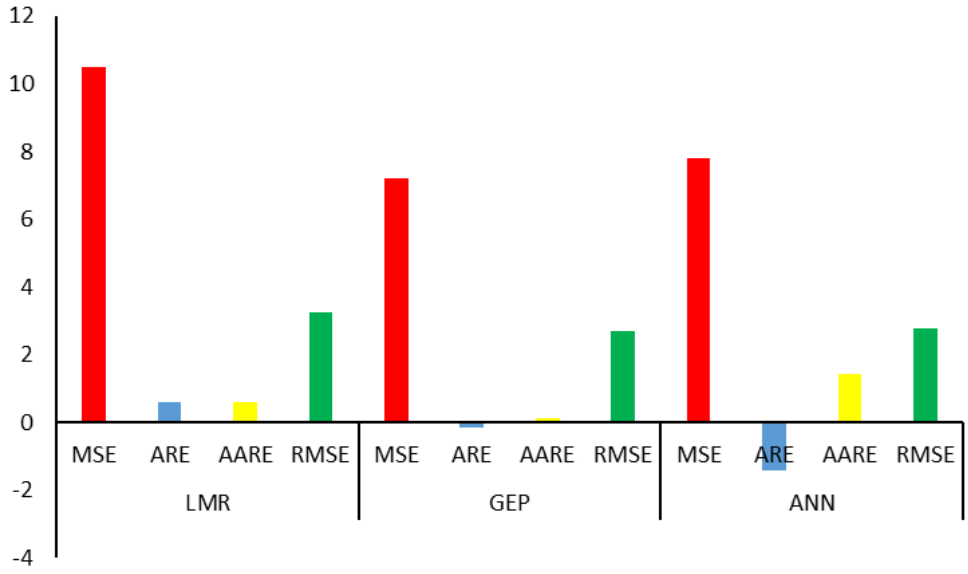

Fig. 10. Comparison of the statistical parameters for predictions of LMR, ANNs, and GEP models

the tornado sensitivity analysis, the range of the correlations is between –1 and +1. Figure 11 shows the tornado analysis for the PPV. As it is shown in this figure, the distance to blasting block and the charge per delay are the most effective parameters on the PPV. It is obvious that unlike the distance to blasting block, with increasing the amount of the charge in each delay, the PPV increases dramatically.

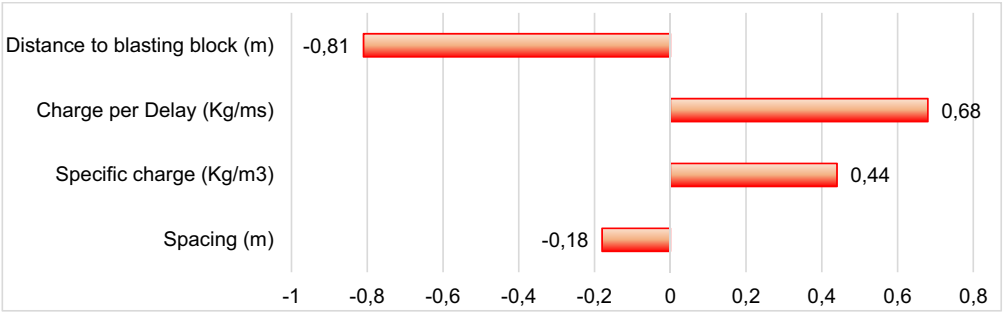

Fig. 11. Sensitivity analysis with using the tornado diagram

Based on the nature of the blasting operation, eliminating the BIGV is not possible, but for decreasing this phenomenon it is recommended that the following activities were considered:

- As the distance to the blasting block is the most effective parameter on the PPV, the buildings should be constructed behind the affected area.
- Using suitable delay timing can efficiently decrease the PPV level. Delay timing decreases the maximum charge per each blasting sequence. In other words, suitable delay timing decreases the blasting volume from the whole block to a blast hole.
- As an obvious rule of thumb, it is important that the specific charge kept in the acceptable range. For this purpose, it is necessary to clean the front of the blasting face, leveling the surface, eliminating the water in the blast holes, etc.

8. Conclusions

The vibration is an inevitable consequence of blasting, which can impose damages to the structures, such as buildings, bridges, dams, tunnels, etc. Therefore, the blast-induced ground vibration (BIGV) and its propagation throughout the rock masses must be carefully regarded to eliminate (or at least minimize) the risk of damage to nearby structures. In the present study, an attempt was made to predict the ground vibration using the LMR, the ANNs and the GEP. For this purpose, the data on the distance to the blasting block, burden, spacing, specific charge, and charge per delay were considered as input parameters, with the actual values taken from the blasts at the Sarcheshmeh copper mine. Once finished with developing various models for predicting the PPV, some performance indicators were calculated to evaluate the proposed prediction models, including R-square, RMSE, and MSE. The results showed that the developed GEP could practically outperform the LMR. Taking MSE as the objective function, the obtained values of R-square and RMSE using the GEP algorithm for predicting the PPV indicated higher accuracy of this algorithm compared to the LMR and the ANNs. The obtained values of R-squared and RMSE corresponding to GEP were 0.91 and 2.67, respectively, while those of LMR were 0.70 and 3.18, respectively. Also, the lower values of R-Squared and RMSE, 0.88 and 2.81, for the ANNs results proved that the GEP was more reliable and more reasonable.

References

[1] M. Khandelwal, T.N. Singh, *Prediction of blast induced ground vibrations and frequency in opencast mine: a neural network approach*. Journal of Sound and Vibration **289** (4-5), 711-725 (2006).

[2] R.S. Faradonbeh, D.J. Armaghani, M.A. Majid, M.M. Tahir, B.R. Murlidhar, M. Monjezi, H.M. Wong, *Prediction of ground vibration due to quarry blasting based on gene expression programming: a new model for peak particle velocity prediction*. International Journal of Environmental Science and Technology **13** (6), 1453-1464 (2016).

[3] M. Monjezi, M. Ghafurikalajahi, A. Bahrami, *Prediction of blast-induced ground vibration using artificial neural networks*. Tunnelling and Underground Space Technology **26** (1), 46-50 (2011).

[4] S.R. Dindarloo. *Prediction of blast-induced ground vibrations via genetic programming*. International Journal of Mining Science and Technology **25** (6), 1011-1015 (2015).

[5] M. Hajihassani, D.J. Armaghani, M. Monjezi, E.T. Mohamad, A. Marto, *Blast-induced air and ground vibration prediction: a particle swarm optimization-based artificial neural network approach*. Environmental Earth Sciences **74** (4), 2799-2817 (2015).

[6] D.J. Armaghani, E. Momeni, SVANK. Abad, M. Khandelwal, *Feasibility of ANFIS model for prediction of ground vibrations resulting from quarry blasting*. Environmental Earth Sciences **74** (4), 2845-2860 (2015).

[7] M. Hasanipanah, S.B. Golzar, I.A. Larki, M.Y. Maryaki, T. Ghahremanians, *Estimation of blast-induced ground vibration through a soft computing framework*. Engineering with Computers **33** (4), 951-959 (2017).

[8] R.S. Faradonbeh, M. Monjezi, *Prediction and minimization of blast-induced ground vibration using two robust meta-heuristic algorithms*. Engineering with Computers **33** (4), 835-851 (2017).

[9] H. Sheykhi, R. Bagherpour, E. Ghasemi, H. Kalhori, *Forecasting ground vibration due to rock blasting: a hybrid intelligent approach using support vector regression and fuzzy C-means clustering*. Engineering with Computers **34** (2), 357-365 (2018).

[10] S. Stanković, M. Dobrilović, V. Škrlec, *Optimal positioning of vibration monitoring instruments and their impact on blast-induced seismic influence results*. Archives of Mining Sciences **64** (3), 591-607 (2019).

[11] P. Mertuszka, M. Szumny, K. Fulawka, J. Maslej, D. Saiang, *The Effect of the Blasthole Diameter on the Detonation Velocity of Bulk Emulsion Explosive in the Conditions of the Rudna Mine*. Archives of Mining Sciences **64** (4), 725-737 (2019).

[12] AI. Lawal, M.A. Idris, *An artificial neural network-based mathematical model for the prediction of blast-induced ground vibrations*. International Journal of Environmental Studies 1-17 (2019).

[13] D.C. Montgomery, E.A. Peck, *Introduction to Linear Regression Analysis Wiley*. New York, USA (1992).

[14] C. Ferreira, *Gene expression programming: a new adaptive algorithm for solving problems*. arXiv preprint cs/0102027. (2001).

[15] H. Dehghani, *Forecasting copper price using gene expression programming*. Journal of Mining and Environment **9** (2), 349-360 (2018).

[16] I.S. Alkroosh, P.K. Sarker, *Prediction of the compressive strength of fly ash geopolymer concrete using gene expression programming*. Computers and Concrete **24** (4), 295-302 (2019).

[17] X.Y. Wang, *Optimal design of the cement, fly ash, and slag mixture in ternary blended concrete based on gene expression programming and the genetic algorithm*. Materials **12** (15), 2448 (2019).

[18] B. Jodeiri Shokri, H.R. Ramazi, F. Doulati Ardejani, M. Sadeghiamirshahidi, *Prediction of pyrite oxidation in a coal washing waste pile applying artificial neural networks (ANNs) and adaptive neuro-fuzzy inference systems (ANFIS)*. Mine Water and the Environment **33**, 146-156 (2014).

[19] H. Dehghani, M. Ataee-pour, *Development of a model to predict peak particle velocity in a blasting operation*. International Journal of Rock Mechanics and Mining Sciences **48** (1), 51-58 (2011).

[20] H. Rezaee, M. Asghari, *Accounting for secondary variable for the classification of mineral resources using cokriging technique; a case study of Sarcheshmeh porphyry copper deposit*. International Journal of Mining and Geo-Engineering **45** (1), 67-69 (2011).

[21] M. Pishbin, N. Fathianpour, *Assessing the performance of statistical-structural and geostatistical methods in estimating the 3d distribution of the uniaxial compressive strength parameter in the Sarcheshmeh porphyry copper deposit*. Journal of Mining and Environment **48** (1), 11-30 (2014).